

Rapid #: -23815371

CROSS REF ID: **1385556**

LENDER: **S9V (University of the Sunshine Coast) :: Main Library**

BORROWER: **ORE (Oregon State University) :: Main Library**

TYPE: Article CC:CCG

JOURNAL TITLE: Nuclear science and engineering

USER JOURNAL TITLE: Nuclear science and engineering : the journal of the American Nuclear Society.

ARTICLE TITLE: Multiphysics Modeling of Heat Pipe Microreactor with Critical Control Drum Position Search

ARTICLE AUTHOR: Price, Dean

VOLUME:

ISSUE:

MONTH: 11

YEAR: 2024

PAGES: 1-20

ISSN: 0029-5639

OCLC #:

Processed by RapidX: 1/16/2025 4:28:12 PM

Commonwealth of Australia

Copyright Act 1968

Notice for paragraph 49 (7A) (c) of the Copyright Act 1968

WARNING

This material has been provided to you under section 49 of the Copyright Act 1968 (the Act) for the purposes of research or study. The contents of the material may be subject to copyright protection under the Act,

Further dealings by you with this material may be a copyright infringement. To determine whether such a communication would be an infringement, it is necessary to have regard to the criteria set out in Division 3 of Part III if the Act.

Do not remove this notice



Multiphysics Modeling of Heat Pipe Microreactor with Critical Control Drum Position Search

Dean Price, Nathan Roskoff, Majdi I. Radaideh & Brendan Kochunas

To cite this article: Dean Price, Nathan Roskoff, Majdi I. Radaideh & Brendan Kochunas (04 Nov 2024): Multiphysics Modeling of Heat Pipe Microreactor with Critical Control Drum Position Search, Nuclear Science and Engineering, DOI: [10.1080/00295639.2024.2409582](https://doi.org/10.1080/00295639.2024.2409582)

To link to this article: <https://doi.org/10.1080/00295639.2024.2409582>



Published online: 04 Nov 2024.



Submit your article to this journal 



Article views: 123



View related articles 



View Crossmark data 



Multiphysics Modeling of Heat Pipe Microreactor with Critical Control Drum Position Search

Dean Price,^{10, a*} Nathan Roskoff,^b Majdi I. Radaideh,¹⁰ and Brendan Kochunas¹⁰^a

^a*University of Michigan, Department of Nuclear Engineering and Radiological Science, 2355 Bonisteel Boulevard, Ann Arbor, Michigan 48109*

^b*Westinghouse Electric Company LLC, 1000 Westinghouse Drive, Cranberry Township, Pennsylvania 16066*

Received March 2, 2024

Accepted for Publication August 8, 2024

Abstract — *A multiphysics coupling methodology for heat pipe microreactors is presented in this work that includes a focus on a critical control drum position search routine and burnup capabilities. As the Serpent code is used for neutronics calculations, the recently developed GRsecant method for finding critical control drum positions is employed, which has explicit measures to manage the uncertainty introduced from the Monte Carlo calculation method. This work complements existing multiphysics modeling tools for heat pipe microreactors because it can be used to generate cross sections with fuel compositions determined by depletion with critical control drum positions.*

These methods are applied to a microreactor design motivated by the eVinci™ heat pipe microreactor. The convergence of the multiphysics coupling routine is analyzed at multiple burnup points. The multiphysics iterations with critical control drum search were observed to converge for all calculations performed in this work. Overall, the multiphysics coupling procedure enables the calculation of both thermal and neutronics characteristics with control drums in their critical positions for the core lifetime.

Keywords — *Multiphysics, microreactor, control, heat pipe, eVinci.*

Note — *Some figures may be in color only in the electronic version.*

I. INTRODUCTION

The development of nuclear microreactors will enable nuclear power to serve unique economic markets that have previously been inaccessible to larger, more expensive nuclear power plants.^[1] The development of these reactors also increases the need for computational simulations that enable efficient design and analysis. One method of computational simulation that minimizes the reliance of an analysis framework on operational data is multiphysics simulations. These methods are

particularly important for microreactor design and analysis because, currently, microreactor operational data is limited.

One paper that provides some discussion on multiphysics simulation in the context of nuclear engineering defines them as “simulations which include some level of disparate physical phenomena.”^[2] Generally, these simulations are comprised of some combination of codes that simulate neutronics (the generation and transport of neutrons), thermal hydraulics (the transfer of heat and mass), and fuel performance (the deformation and thermomechanics of solid materials with consideration of other effects like fission gas release and species diffusion).

*E-mail: deanrp@umich.edu

The Multiphysics Object Oriented Simulation Environment (MOOSE) is a multiphysics coupling software developed at Idaho National Laboratory that can be used to perform simulations for a variety of nuclear reactor systems through the use of many subapplications.^[3] One example of a microreactor multiphysics simulation workflow that is enabled by MOOSE is DireWolf. DireWolf is used to specifically simulate heat pipe-cooled microreactors and is capable of simulating neutron transport, fuel performance, thermal hydraulics, and structural mechanics.^[4]

The main code used to solve the neutron transport equation in the DireWolf code for thermal reactors is Griffin.^[5] The transport solver in Griffin uses the preconditioned Jacobian-free Newton-Krylov method^[6] to solve for the fundamental mode of the eigenvalue approximation applied to the multigroup neutron transport equation over a finite element mesh with the quasi-static method^[7] for transient simulations. Griffin typically requires precomputed multigroup cross-section libraries that can be generated with the Serpent 2^[8] Monte Carlo neutronics code.

The next primary constituent of the DireWolf code is Sockeye,^[9] which is used to simulate the physics of heat pipes. Although Sockeye is capable of more advanced fluid models to accurately capture the heat and mass transfer in heat pipes, Berry et al.^[9] showed that simpler thermal network-based models are accurate for steady-state operation.^[10] The final primary constituent of DireWolf is Bison,^[11] which is used to perform the thermomechanical analyses associated with the heat pipe microreactor. In the application of DireWolf to the Empire reactor design,^[12] which was published in Ref. [4], Bison was used to calculate heat conduction and elastic strain. DireWolf was demonstrated on reactor design when it was used to simulate the eVinci^{TMa} microreactor in steady-state^[13] and transient operations.^[14]

In general, many studies have generated multiphysics analysis methodologies using custom data passing routines in the analysis of light water reactors (LWRs). Many of these multiphysics tool employ deterministic solvers for the neutron transport equation. Examples include the VERA-CS (Virtual

Environment for Reactor Applications Core Simulator),^[15] which employs MPACT^[16] and nTracer,^[17] both of which use a two-dimensional/one-dimensional method for neutron transport based on the method of characteristics for radial variables and lower-order transport for axial variables.

The use of Monte Carlo methods for neutron transport in these multiphysics coupling methodologies introduces some complexities. One study coupled the Monte Carlo transport code Serpent and OpenFOAM to carry out burnup calculations for 1 year of burnup on a pressurized water reactor pin cell.^[18] In this study, three challenges for multiphysics coupling with Monte Carlo codes were specifically identified:

1. high computational cost
2. convergence and numerical instabilities in the coupling algorithms between the various physical simulations
3. local burnup instabilities induced from neutronics and coupled depletion.

Challenge 1 is relatively straightforward and challenge 2 is elaborated on in Ref. [19], where a mathematical description of stability in the context of neutronics–thermal-hydraulics coupling is provided. Additionally, Ref. [20] provides some discussion on coupling with Monte Carlo methods and an exploration into the stability of the coupling procedure. Finally, challenge 3 is concisely described in Ref. [21], with some exploration with a pin cell numerical model.

Moving forward, work has also been done in multiphysics coupling for microreactors outside of the MOOSE framework. Im et al.^[22] demonstrated the coupling of PRAGMA, OpenFOAM, and ANLHTP to simulate a heat pipe microreactor. This study provided an in-depth discussion on run-time metrics and implementation details for the multiphysics model, as well as a demonstration of both normal operating conditions and heat pipe failure conditions. Although the aforementioned challenge 1 was thoroughly addressed through the graphic processing unit utilization capabilities in PRAGMA, and the instabilities described in challenge 2 seemed to not affect the results, the lack of burnup analysis makes challenge 3 irrelevant.

In another study, Mehta et al.^[23] used MCNP and Abaqus to perform a multiphysics analysis of a hydride-moderated microreactor. The primary focus of their work was to show how the migration of hydrogen during

^aeVinci is a trademark or registered trademark of Westinghouse Electric Company LLC, its affiliates and/or its subsidiaries in the United States of America and may be registered in other countries throughout the world. All rights reserved. Unauthorized use is strictly prohibited. Other names may be trademarks of their respective owners.

operation can affect the neutronics behavior of the core. In Ref. [24], transient simulations were performed with a custom heat pipe code, three-dimensional heat conduction with ANSYS FLUENT, and a point kinetics model. With this multiphysics methodology, steady-state, startup, and heat pipe failure operations were modeled without the use of Monte Carlo methods.

Even with a thorough exploration of multiphysics coupling in both MOOSE and other software, there is still a gap in the consideration of reactivity control during burnup analysis in these multiphysics methodologies. The main shortcomings of DireWolf in this respect comes from its reliance on separate cross-section generation. Alternatively, both Refs. [22,23] provide minimal discussion on the treatment of control drum positions during burnup analysis. The current study has a novel component in that it includes an iterative critical drum position search procedure within the Picard iterations used to find the converged multiphysics solution. This permits burnup calculations to be performed on the core with control drum positions that maintain core criticality.

Overall, the current study seeks to complement existing multiphysics modeling methodologies by coupling a Monte Carlo-based neutron transport solver directly to the other physical simulations. This coupling approach can be seen in another MOOSE tool, Cardinal.^[25] In the current state of Cardinal, this approach removes the capability to perform transient simulations, but enables the high-fidelity simulation of the full cycle without any need for geometry homogenization or energy condensation, with the latter being important for correctly modeling scattering and leakage in the system.

The current work presents the application of a multiphysics coupling procedure that uses OpenFOAM^[26] to solve the heat diffusion equation in the solid regions of the core, Serpent^[8] to solve the neutron transport equation, and a thermal network approach to model the heat transfer behavior of the heat pipes. This coupling procedure also includes a control drum critical search routine based on the GRsecant method.^[27] Specific discussion will be given to the aforementioned challenges associated with multiphysics modeling identified in Ref. [18]. Finally, the design used in this study was based on the eVinci microreactor currently under development at Westinghouse Electric Company LLC.^[28] This was done to ensure that the work is relevant to industry efforts in microreactor development.

The remainder of this paper is structured with a methodology section that includes a summary of the design specifications of the reactor used in this study followed by some modeling details about both the

neutronics and thermal modeling. Next in the methodology section, a detailed discussion on the multiphysics calculation procedure and its integration into a burnup analysis procedure is provided. Following the methodology section, the results involving the multiphysics solution with control drums in a fixed position are presented. Then, two subsections are provided on the critical drum search procedure, including multiphysics feedback. The final two subsections in the results section provide the results and a discussion involving the burnup analysis with critical drum positions.

II. METHODOLOGY

II.A. eVinci Motivated Design

The methods in this work are demonstrated on a microreactor design that is similar to the eVinci microreactor. This design, which was created such that this analysis would be nonproprietary, is referred to as the eVinci motivated design (EMD) for the remainder of this paper. Nevertheless, the EMD microreactor has a graphite moderator and a beryllium oxide reflector and is fueled with uranium oxycarbide tri-structural isotropic (TRISO) particles. Reactivity control for the burnup and design transients is provided with a set of 12 control drums located around the core periphery, and shutdown capabilities are enabled with a set of 7 control rods. In this work, the core has a steady-state power output of 4 MW(thermal).

Figure 1 provides the general layout of the core with labeled components. More details on the design, including the dimensions and material specifications, are provided in Ref. [29]. Additionally, Fig. 2 shows how the different control drum angles were represented in the reactor. In this work, all drums moved together such that a single control drum angle could be used to describe the positions of all drums in the core. Furthermore, the alternating directions of positive rotation were used to allow for 1/12 symmetry to be applied to the simulation models.

II.B. Neutronics Model

One major component of the multiphysics simulation of the EMD microreactor was the modeling of the neutron flux distribution in the core. In this work, the Serpent code^[8] was used to solve the continuous-energy neutron transport equation to obtain the pin power distributions, which are passed to the thermal modeling routine. Additional discussion of the Monte Carlo

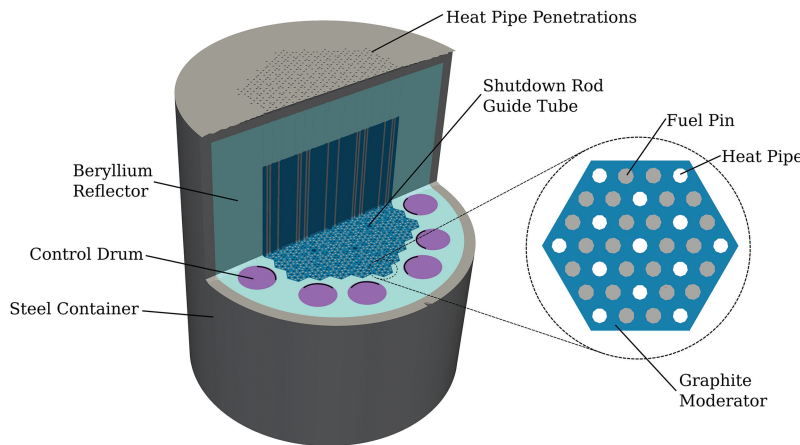


Fig. 1. Layout of EMD microreactor with labeled components. A fuel flake is enlarged to show the layout of the fuel pins and heat pipes. The heat pipes themselves are not shown.

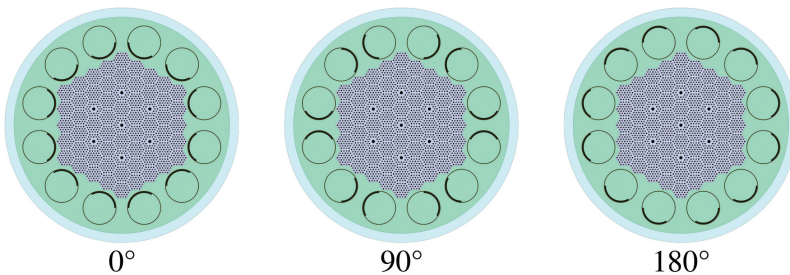


Fig. 2. Control drum configurations with labeled control drum angles.

solution method for the neutron transport equation can be found in Ref. [30].

Being a Monte Carlo code, the number of particle histories or uncertainty in the final eigenvalue is reported alongside the results discussed in Sec. III. However, for applications involving burnup analyses, this uncertainty is an incomplete description of the total uncertainty associated with any calculated quantity because the uncertainty in the cellwise reaction rates are not propagated through the Bateman equations to affect subsequent burnup steps. This shortcoming of the reported uncertainties due to the Monte Carlo calculation method leads to the aforementioned challenge 3, identified by Castagna et al.^[18], being difficult to detect because the code-reported uncertainties cannot be used to identify the instability.

With success, existing work on the complete propagation of Monte Carlo-induced uncertainties through burnup analyses has relied on backward Euler in place of the matrix exponential to solve the Bateman equations such that the stochasticity in the transition matrix only needs to be propagated through a series of linear operations instead of a matrix exponential.^[31] Also with

success, other work has used perturbation methods^[32] to treat a more general problem where stochasticity comes from both uncertainty in cross sections as well as from the flux solution.

A similar perturbation-based method was employed by Takeda et al.^[33] Also, Tohjoh et al.^[34] developed an analytical method for propagating error in reaction rates through the Bateman equations, but the method was only applicable to some isotopes. Dumonteil and Diop^[35] emphasized the importance of this problem by showing that ignoring the uncertainties in ϕ leads to biases in nuclide concentrations because of the nonlinear nature of the exponential operator. This existing body of work both demonstrates the importance and difficulty of this problem.

In this work, the impact due to the accumulation of Monte Carlo-induced errors on the results were minimized by first limiting the number of axial depletion cells per fuel pin to three. This depletion mesh therefore tracked the fuel composition of three sections of each fuel pin separately. Although some accuracy in the results was lost, the minimization of axial divisions for pinwise depletion cells ensured that each depletion region was

more adequately sampled compared to depletion schemes with more axial divisions.

Additionally, a second measure was taken using a predictor-corrector method with constant extrapolation and linear interpolation as the time integration scheme for the burnup calculations. This effectively doubled the calculation time per burnup step, but encouraged stability throughout the depletion calculation. No radial or azimuthal divisions were used. Therefore, all TRISO particles within each third of each fuel pin were modeled to have the same isotopic composition.

Moving on to other characteristics of the neutronics model, the Monte Carlo calculation method circumvents the need to represent the problem geometry with an unstructured mesh. This enables the explicit representation of a distribution of TRISO particles in the fuel compacts. The ENDF/B-VII.1^[36] cross-section library was used for all calculations. Also, the depletion of the control drum materials was not considered as it was negligible, only fuel materials were depleted. The 1/12 symmetry of the reactor geometry was exploited in the Serpent model by reducing the total number of depletion cells and pin power tally regions.

The unstructured mesh associated with the temperature distribution calculated in OpenFOAM was overlayed on the constructive solid geometry representation of the core contained in Serpent. The calculation of this temperature distribution and its associated mesh is discussed in Sec. II.C. This led to a few low-impact modeling aspects that may be of interest. First, due to the limitations in OpenFOAM that only allow for the treatment of first-order elements in unstructured meshes, curved surfaces were represented by a series of flat surfaces, which led to minor misalignments between the unstructured mesh and the Serpent geometry. Additionally, pin powers were rescaled to allow for conservation of power despite any volumetric differences between these two geometric representations. This misalignment was thought to be superior to a total unstructured mesh representation of the core geometry in Serpent, which would lose both the ability to explicitly represent TRISO particles and curved surfaces.

Second, the control rod guide tubes were not modeled in the OpenFOAM model, and therefore, were set to a constant temperature of 300 K in the Serpent model. This may lead to minor inaccuracies in the neutron flux in local regions around the control rod guide tubes. Future work will more carefully select this constant temperature to minimize these inaccuracies. Finally, the TRISO particles were not explicitly represented in the OpenFOAM mesh. Therefore, the temperatures from the homogenized fuel region in the OpenFOAM mesh were overlayed on

the heterogeneous fuel regions containing TRISO particles in the Serpent geometry. This caused all layers of the TRISO particles and the surrounding graphite in the fuel pin region to be the same temperature.

II.C. Thermal Model

The thermal modeling component of this methodology, which was fairly complex, has been separately published in Ref. [29]. Therefore, a brief discussion of the thermal modeling methods is presented here. To begin, the chtMultiRegionFoam solver in OpenFOAM was used for this analysis,^[26] with the semi-implicit method for pressure-linked equations (SIMPLE) algorithm used to solve the steady-state heat transfer equation using a pseudo time-stepping scheme.^[37]

In this study, OpenFOAM was only used to treat the solid regions of the core, where the heat pipes were simulated separately and coupled using boundary conditions at the boundary defined by the interface between the outer wall of the heat pipe and the inner surface of the moderator, reflector, or container. A multiregion form of Poisson's equation was the governing equation for calculating the heat transfer in the solid regions of the core. Meshing was performed with gmsh, an open-source meshing software.^[38] A characteristic mesh length of 0.6 cm was used in the current work; it is illustrated in the Appendix of Ref. [29].

The OpenFOAM model was based on a 1/12 symmetry of the EMD microreactor, with the absorbing region of the control drums replaced with BeO to simplify the model. This change had a minimal impact on the core temperature distributions in the fueled region of the core.

Additionally, perfect gap conductance (no thermal insulance) between all material regions within the OpenFOAM model was assumed. This assumption may impact the convergence characteristics of the multiphysics methods discussed in this work. To explain, thermal insulances will tend to exaggerate the temperature changes with respect to changes in power. This more significant reactivity feedback could lead to instability. All heat generation was contained within the fuel pin regions.

Convection boundary conditions were used on the outsides of the stainless steel container with an ambient temperature of 298 K and an arbitrarily selected convective heat transfer coefficient of 5 W/m²·K. Although the results in this paper show some sensitivity to this outer boundary condition, the majority of the power in the core was extracted by the heat pipes, which minimized the impact of this outer boundary condition. Additional discussion on the convective heat transfer and its representation as a boundary condition can be found in Part III of Ref. [39].

An adiabatic boundary condition was used at the interface of the shutdown rod guide tubes and the graphite moderator. From the neutronics calculation, each fuel pin was split into 11 axial zones in which the pin power was tallied. In the OpenFOAM model, this led to each pin being split into 11 axial zones with a constant heat generation rate within them. Note that these 11 axial divisions, on which the pin power was tallied for thermal calculations, were separate from the 3 axial divisions used for the depletion cells. The constitutive models used for thermal conductivities and heat capacities are discussed in Ref. [29].

The second portion of the thermal modeling methodology consisted of heat pipe modeling, which is discussed in mathematical detail in Ref. [29]. In this work, the vapor core region of each heat pipe was modeled as a thermal superconductor with a thermal circuit, or network, model. Figure 3 shows how this thermal circuit is representative of the physical heat pipe system. Mueller and Tsvetkov^[10] presented a review of various modeling techniques of heat pipes for microreactors and demonstrated that this was a relatively good approximation, particularly when modeling reactors in steady state.

The strength of the isothermal vapor core approximation was demonstrated in Ref. [40], where the axial vapor temperature distributions were shown to vary less than 1 K over the length of the heat pipe during a startup transient. Referred to as an iterative vapor temperature boundary condition in Ref. [29], this thermal circuit model required an iterative procedure that first solved for the heat pipe vapor core temperatures using

a closed-form explicit equation that relied on the surface-integrated heat flux at the interface between the graphite moderator and heat pipe. Then the boundary condition was updated in the OpenFOAM model and the full-core temperature distribution was updated.

II.D. Multiphysics Coupling

II.D.1. Steady-State Calculation

A calculation flow map that shows the quantities exchanged between the various components of the multiphysics coupling procedure is provided in Fig. 4. This flow map only describes the process for obtaining the steady-state behavior of the core. The incorporation of this procedure into burnup calculations is discussed in Sec. II.D.2.

The steady-state multiphysics coupling procedure begins by assuming a flat pin power distribution $q(\mathbf{x})$ is constant in the fuel pins. Then the thermal calculation is initiated by also assuming uniform heat pipe vapor core temperatures across all heat pipes and solving for the temperature distribution in the solid region of the core. Periodically, throughout the iterations of the SIMPLE algorithm, specifically every 100 iterations, the heat flux at the outer boundary of each heat pipe is integrated $\int_S q''(\mathbf{x})dS$ and used to update the heat pipe vapor core temperatures T_{vap} . A relaxation factor of 0.5 was used when updating the heat pipe vapor core temperatures.

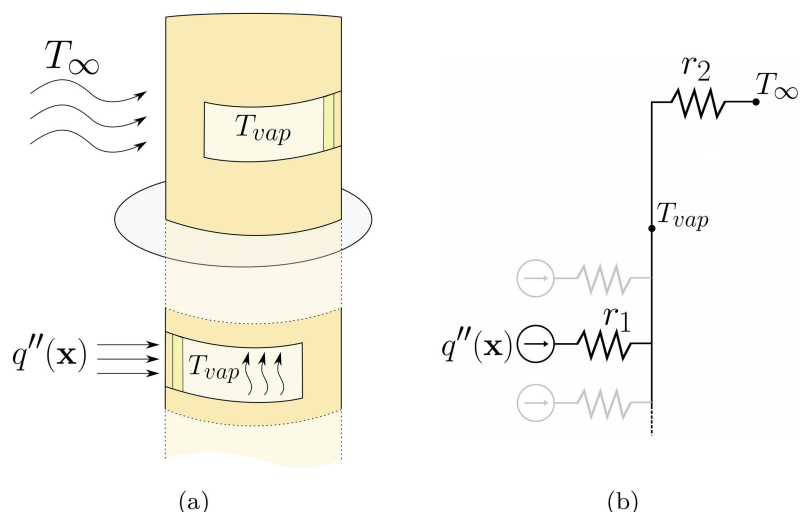


Fig. 3. (a) Heat pipe diagram with evaporator and condenser regions to depict how some heat flux incident on the surface of the pipe at x is transported out of the core. (b) The representative thermal circuit in terms of heat flux (as opposed to heat rate) approximates the heat transport behavior illustrated in (a) with two insulations: r_1 and r_2 . This figure was originally published in Ref. [29].

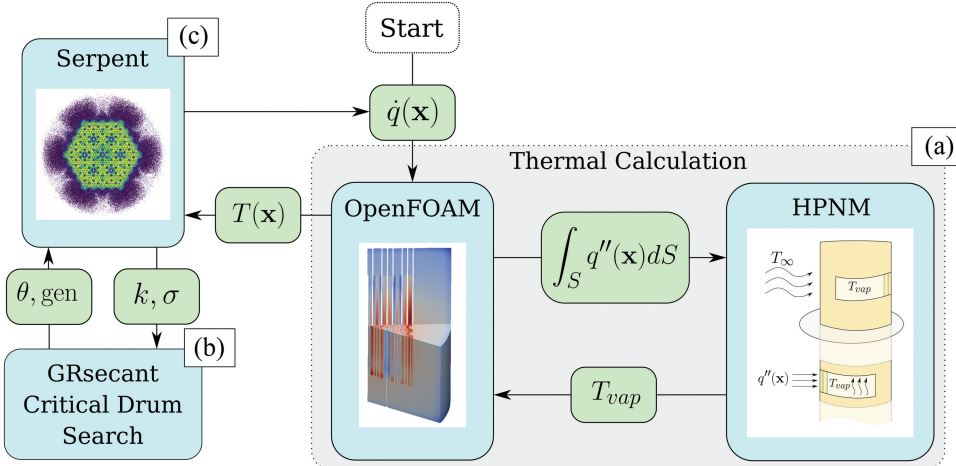


Fig. 4. Exchange of calculated quantities between various components of the multiphysics coupling procedure for steady-state operation. Each component is labeled with (a), (b), or (c) to show the procedural progression through the various components.

These two iterative parameters were explored more thoroughly in Ref. [29], where it was found that more SIMPLE algorithm iterations between heat pipe vapor temperature updates led to more stability. To simplify the flow map in Fig. 4, the convergence criteria are not shown. However, termination of the thermal calculation required the satisfaction of two convergence criteria. First, 800 total iterations of the SIMPLE algorithm had to be performed. Second, the maximum change in the vapor temperature between two iterations across all heat pipes $\epsilon_{T_{vap}}$ should be less than 1 K. As the computational cost of the thermal calculation was small compared to the computational cost of the Serpent calculation, this convergence criterion was selected to be fairly strict due to its small impact on the total computational cost of this procedure.

All thermal calculations used in this work were terminated upon reaching the minimum 800 iterations of the SIMPLE algorithm; none required additional iterations to satisfy the second convergence criteria. This led to the specific selection of $\epsilon_{T_{vap}} \leq 1$ K to have no impact on the results. A more in-depth discussion on the thermal calculation procedure and the selection of various iterative parameters is given in Ref. [29]. Additionally, more discussion on the potential instabilities associated with challenge 2, identified by Castagna et al.,^[18] are discussed in Ref. [29].

The converged core temperature distribution was then incorporated into the Serpent model on an unstructured mesh. One additional feature in the multiphysics coupling procedure used in the current study was that the GRsecant method, originally presented in Ref. [27], was used to update the control drum angle θ and the number

of histories gen to run with every Serpent calculation. This GRsecant method requires both the core multiplication factor k and the current estimate in the uncertainty in the core multiplication factor σ due to the Monte Carlo calculation method. The GRsecant method is a stochastic root-finding algorithm specifically created for this application. In earlier iterations of the multiphysics coupling procedure, fewer neutron histories were used to calculate core characteristics while exploring control drum positions, which did not yield a critical core. As the root-finding algorithm progressed, more neutron histories were run per iteration.

In order for the full iterative procedure to calculate steady-state core characteristics with critical control drum positions, three parameters must be set. First, two convergence criteria were selected: (1) the final proximity of core multiplicity to critical and (2) the final uncertainty in the calculated core multiplicity. In all results in this work, the final proximity of core multiplicity to critical was selected to be 100 pcm. Second, the final uncertainty in the calculated core multiplicity was selected to be 20 pcm. Deeper exploration into the selection of these parameters may be warranted, but for this study, the final 20 pcm uncertainty in the core multiplicity was selected for sufficient statistics on the axial pin power distribution and 100 pcm from the core criticality led to control drum positions generally within 1 deg of the critical control drum searches performed with much stricter convergence criteria.

The third parameter that must be selected is the number of thermal/neutronics iterations to be run following the satisfaction of the previous two convergence criteria. These additional iterations ensure the convergence of the coupled thermal physics of the core without a changing

control drum position. In the current work, only one additional iteration was run because of the relatively fast convergence observed in Sec. III.A for fixed-position iterations.

In reference to challenge 2 mentioned by Castagna et al.^[18], the neutronics and thermal iterations were found to be stable in all analyses. Although the negative, and relatively linear, relationship between the neutron cross sections and temperature did not guarantee this stability, it tended to encourage stability. However, some instabilities can be introduced by the GRsecant drum search procedure. Further discussed in Ref. [27], the gradient-reliance of the GRsecant algorithm can allow for instabilities in the algorithm caused by the noise arising from the Monte Carlo calculation method of core multiplicities. The GRsecant method has a lower theoretical order of convergence than the conventional secant method, allowing for specific measures taken to minimize the occurrence of these instabilities.

In reference to challenge 1 mentioned by Castagna et al.^[18], the smaller number of neutron histories used in the earlier portions of the multiphysics coupling iterations reduced the amount of computational time dedicated to calculations where the control drums were far from critical. Nevertheless, this methodology still had a significantly higher computational cost compared to single-physics calculations.

Of course, it may be desirable to calculate the steady-state operating characteristics of the reactor core with a set control drum position. In this event, the control drum rotational position update step associated with the GRsecant method can be neglected. Instead, a set number of histories and control drum positions can be used for all

Serpent calculations and convergence of the neutron flux and temperature distributions will be observed.

II.D.2. Burnup Calculations

As illustrated in Fig. 5, the only information about steady-state reactor operation required in the Bateman equations to evolve the reactor fuel composition over some set time period are cellwise reaction rates. At beginning of life (BOL), the multiphysics coupling routine discussed in Sec. II.D.1 was executed with fresh fuel. Upon converging to a critical control drum position and core temperature distribution, the resulting cellwise reaction rates were used to deplete the fuel over a set time period.

A higher-order predictor corrector method with constant extrapolation in the predictor step and linear interpolation in the corrector step was employed in this study to solve the Bateman equations. Due to the large computational cost associated with the multiphysics coupling routine, it may be desirable to avoid updating the core temperature distribution and control drum position, but still adjust the cellwise reaction rates according to the new fuel composition. In this case, a standalone transport calculation can be executed that maintains the temperature distribution and control drum positions from the previous depletion step. This procedure can be repeated until the multiphysics coupling routine can no longer find control drum positions that yield a critical core, which would indicate that the core is no longer operable (i.e., the core is subcritical with all control drums fully withdrawn).

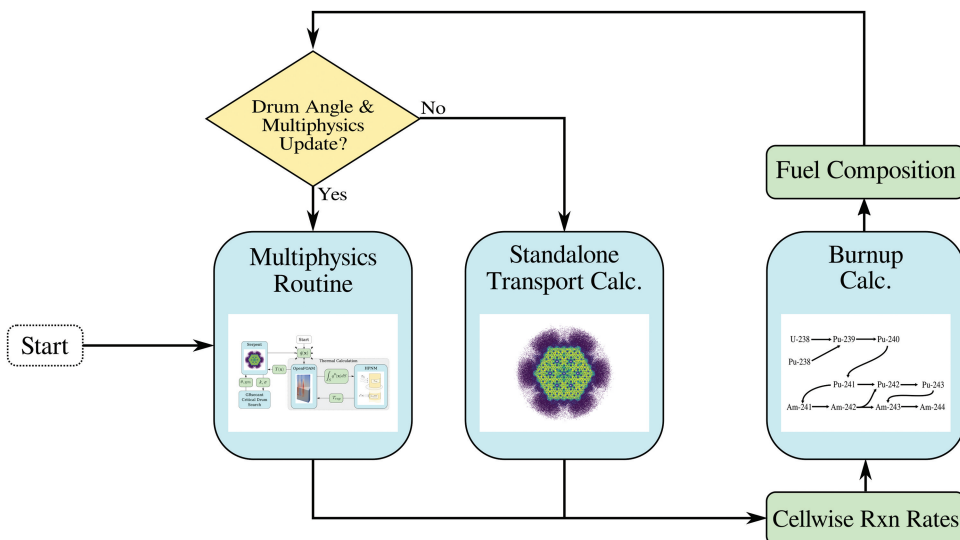


Fig. 5. Burnup calculation routine for depletion with critical control drum positions and thermal.

III. RESULTS

III.A. Fixed Drum Angle Multiphysics

To begin, it is useful to neglect the GRsecant critical drum search routine shown in Fig. 4 and execute a multiphysics coupling procedure with only iterations between the neutronics and thermal simulations. These results can be used to evaluate the stability and convergence characteristics of a more simple multiphysics coupling procedure.

The heat pipe peaking factor (PF), core maximum temperature, k_{eff} , and pin PF are plotted over six iterations between the thermal and neutronics simulations in Fig. 6. The heat pipe PF is the ratio of the maximum core power removed by a single heat pipe to the average core power removed across all heat pipes, and analogously for the pin PF. The heat pipe PF is a highly important design quantity for microreactors because, unlike fuel pins, heat pipes have

both upper and lower power limits for their most efficient operation. A low heat pipe PF indicates that all heat pipes are operating in similar conditions. These quantities are shown for two independent multiphysics coupling procedures executed with control drums fixed fully in their outward-facing positions (180 deg) and fully in their inward-facing positions (0 deg).

As is common in many iterative procedures, the starting configuration of the core should be supplied externally. As such, a constant pin power distribution that led to a total reactor power of about 400 kW (10% of full power) was passed to the initial thermal calculation. This value was selected to deviate from the true full-power operating configuration of the reactor to demonstrate the convergence of the multiphysics coupling procedure with a loosely selected starting point. As such, the selection of the constant pin power distribution led to a suboptimal starting point for the Picard iteration algorithm.

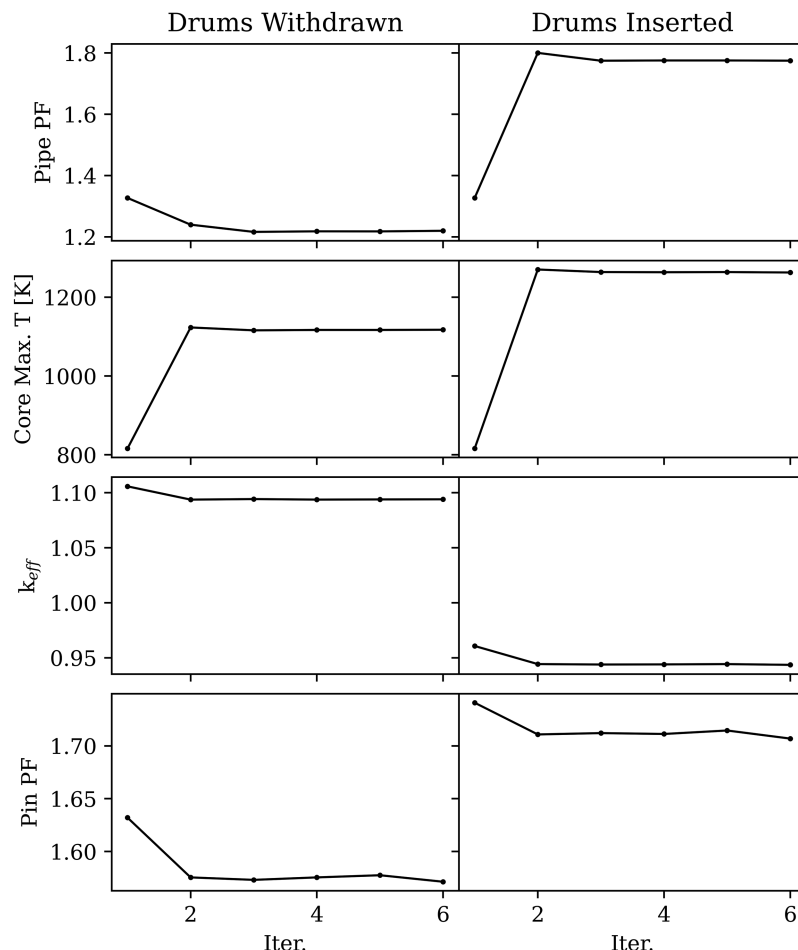


Fig. 6. Convergence of heat pipe PF, core maximum temperature, k_{eff} , and pin PF over multiple Picard iterations in the multiphysics coupling procedure illustrated in Fig. 4 with a fixed control drum position. Uncertainties in k_{eff} due to the Monte Carlo calculation method were too small to show in figure.

Regardless of this selection, all core characteristics quickly converged after a few iterations. Therefore, in most practical analyses, two iterations are likely sufficient to obtain a converged steady-state core configuration for calculations run with a fixed control drum position. The selection of the initial pin power distribution in the thermal calculations was not dependent on control drum position, so quantities that were reported by the thermal calculation at iteration 1 were the same across the two control drum positions. As will be explored later in this section, removal of the drums led to a flatter core power distribution, which led to lower values for the pin PF and maximum core temperature. Naturally, k_{eff} converges to a lower value for the calculations run with the control drum fully inserted.

Figure 7 shows the pin power distributions resulting from the final iteration of the results shown in Fig. 6. On the right side of this figure, the axial power distributions are

calculated with 50 axial divisions in each fuel pin. The noise in these distributions arises from the Monte Carlo calculation method. In the preparation of these axial power distributions for incorporation into OpenFOAM, they were averaged across 11 axial nodes, which reduced the magnitude of this noise by a factor of $\sqrt{50/11} \approx 2.1$.

Consistent with the results shown in Fig. 6, it is clear that the full insertion of the control drums would lead to significantly higher peaking in the core power distribution. Fortunately, the requirement for a shutdown margin at BOL prevents any reactor from operating with the control drums in this position. Therefore, this more severe PF does not impact any design requirements for realistic microreactor designs. Additionally, the moderating effect of the beryllium oxide reflector can be seen in two ways in Fig. 7. First, radially, the fuel pins in Fig. 7a located at the edge of the fueled region have the highest power. This effect is not

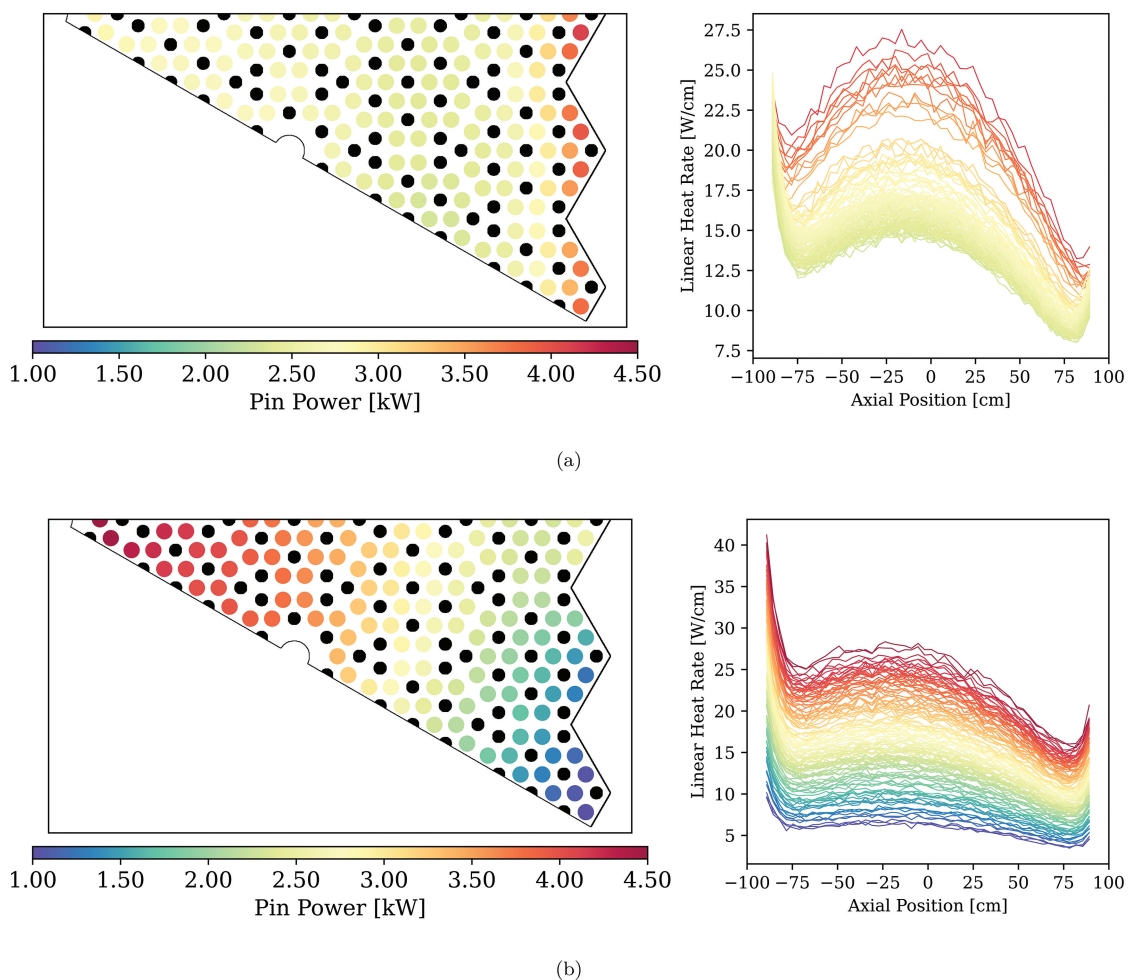


Fig. 7. Radial and axial power distributions resulting from the multiphysics coupling routine with fixed control drum positions with (a) control drums fully withdrawn and (b) control drums fully inserted. Each line in the right portion of each figure represents the axial power distribution of a single pin. These lines keep the color of their position in the radial power distribution plot. The black dots represent heat pipes.

observed in Fig. 7b due to the proximity of the control drum absorbing material. Second, the axial pin power distributions have clear sharp increases at the top and bottom of the fuel pins. The increase in the bottom region of the core is more pronounced due to the absence of heat pipes extending through the bottom reflector.

The steady-state core temperature distribution resulting from the multiphysics coupling procedure executed with the control drums fully withdrawn is shown in Fig. 8. A portion of the temperature distribution was removed to visualize the radial and axial core temperature distribution in the active fueled region. The heat pipes are shown in the cooler areas of the active fueled region.

Due to the presence of heat pipes at all six corners of the fuel flakes, the heat pipes tend to form clusters of three in the active fueled region, which form cold regions at the corners of each fuel flake. Additionally, the high pin powers along the outer radius of the active fueled region cause the highest core temperatures to be located near the reflector region. This effect does not cause high heat pipe temperatures because the heat pipes in these regions tend to not be surrounded by fuel pins like the heat pipes in other core regions. Axially, the core temperatures tend to decrease toward the upper reflector.

Due to the homogenization of the axial pin power distributions into 11 axial sections, the sharp increases in power observed at the upper and lower portions of the

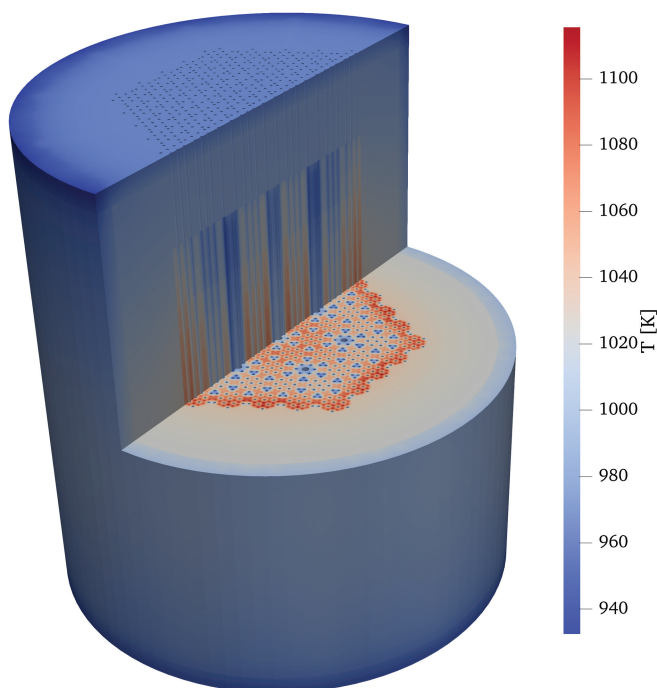


Fig. 8. Steady-state core temperature distribution for BOL with control drums facing outward.

active fueled region observed in Fig. 7 do not cause significant increases in temperature in these same regions. A comparison of this temperature distribution with the temperature distribution calculated with control drums in their critical position is presented in Sec. III.C.

It is additionally useful to compare the total control drum reactivity worth calculated with a multiphysics routine that allows for the inclusion of thermal feedback to the drum reactivity worth calculated using neutronics alone. By comparing k_{eff} from the final iteration of the multiphysics coupling routine, the drum worth was calculated to be $14574 \text{ pcm} \pm 33 \text{ pcm}$, including multiphysics feedback. Without multiphysics feedback, two separate standalone Serpent calculations were run with control drums facing inward and outward. The core temperature distribution was constant between these two calculations. In this calculation, the control drum worth was $14358 \text{ pcm} \pm 26 \text{ pcm}$. The reported uncertainty of these quantities arises strictly from the reported Monte Carlo statistics on k_{eff} values. The consideration of multiphysics feedback only changes the total control drum worth by about 1.5% or 216 pcm.

III.B. Critical Control Drum Search with Multiphysics

The multiphysics coupling procedure shown in Fig. 4 was executed on a fresh fuel composition. The progression of four quantities throughout this search process are shown in Fig. 9. First, $|1 - k_{eff}|$ is plotted over nine iterations. This quantity describes the proximity to core criticality observed throughout the procedure. Figure 9 includes a blue dotted line to show the 100 pcm termination criteria imposed on the problem. Following the eight iterations of the full coupling procedure, a final single iteration was executed without any changes in control drum position. This was done to ensure the convergence of the full multiphysics solution.

Second, the control drum angles are shown. As the first two control drum angles were provided by the user to be 70 deg and 90 deg. As the search progresses, the GRsecant method effectively provided control drum angles that reduced $|1 - k_{eff}|$, causing monotonic convergence. Third, the uncertainty in k_{eff} is also shown in Fig. 9, with the 20 pcm termination criteria shown as a blue dotted line. Similar to the control drum angles, the Monte Carlo sampling parameters associated with the first two calculations in this workflow need to be user defined.

Then, starting on the third iteration, the GRsecant method progressively selects these Monte Carlo sampling parameters to decrease the uncertainty in k_{eff} until the

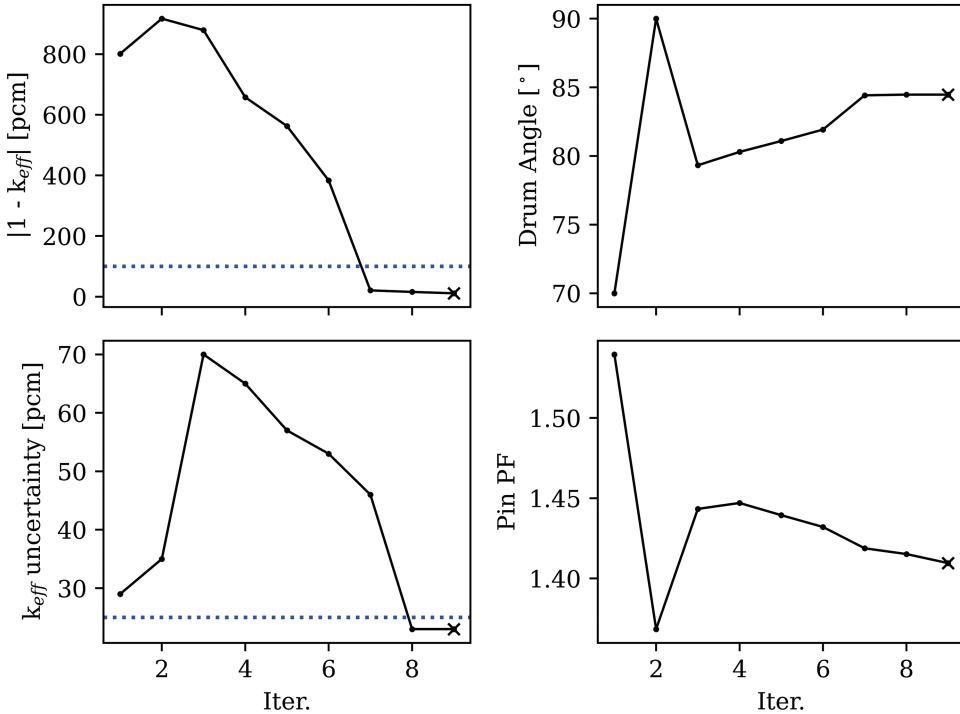


Fig. 9. Quantities resulting from the multiphysics coupling workflow with critical control drum position search. Search termination criteria of 100 pcm in proximity to $k_{eff} = 1$ and 20 pcm in k_{eff} uncertainty are shown as blue dotted lines. The final iteration, indicated by “x” was executed without any update to the control drum position or Monte Carlo sampling parameters.

termination criteria are satisfied. Note how the termination criteria associated with $|1 - k_{eff}|$ were satisfied on iteration seven, but only on iteration eight were both termination criteria satisfied. Finally, the pin PF is provided as some measure of the convergence of the pin power distribution over the coupling workflow. Due to the rapid convergence of the multiphysics solution observed in Fig. 6, only a single additional iteration was run with unchanging control drum positions. Regardless, there was a relatively small change in the calculated pin PF over this final iteration, which the Monte Carlo uncertainty in the pin powers may certainly have contributed to.

Although more discussion on the performance of the burnup routine is provided in Sec. III.D, it is useful to explore the performance of the multiphysics coupling routine with a critical control drum search when the core contains depleted fuel compositions. As such, Fig. 10 shows the progression of the search procedure at different points during the core lifetime. Although the search routine did consistently converge and exhibit generally monotonic reduction in $|1 - k_{eff}|$, the search procedure executed at $t = 1$ year took significantly longer than the search routines performed at other times.

As the Monte Carlo error associated with k_{eff} drives much of the difficulty in the efficient execution of this search routine, the number of iterations required to reach convergence tends to behave randomly. However, in reference to challenge 2 from Ref. [18], the control drum search routine does not notably increase the potential for nonconvergence (assuming a control drum position exists that yields a critical core). Due to the boundedness of the control drum parameter, the imposition of these bounds on the control drum prevents the search routine from progressing to unphysical domains. Nevertheless, the noise from the Monte Carlo calculation method can certainly disrupt the progression of the search procedure and lead to coupling routines that require a large number of iterations.

In reference to challenge 1 from Ref. [18], these multiphysics calculations can take a large amount of time. These calculations were run with 24 processors on Intel® Xeon® CPU E5-2680 v3 CPUs. Figure 11 shows the total computational time dedicated to the Monte Carlo transport solution method in each search routine. The computational time dedicated to the temperature distribution was comparatively negligible. In Fig. 11, the total time dedicated to each of the four executed multiphysics coupling routines is shown.

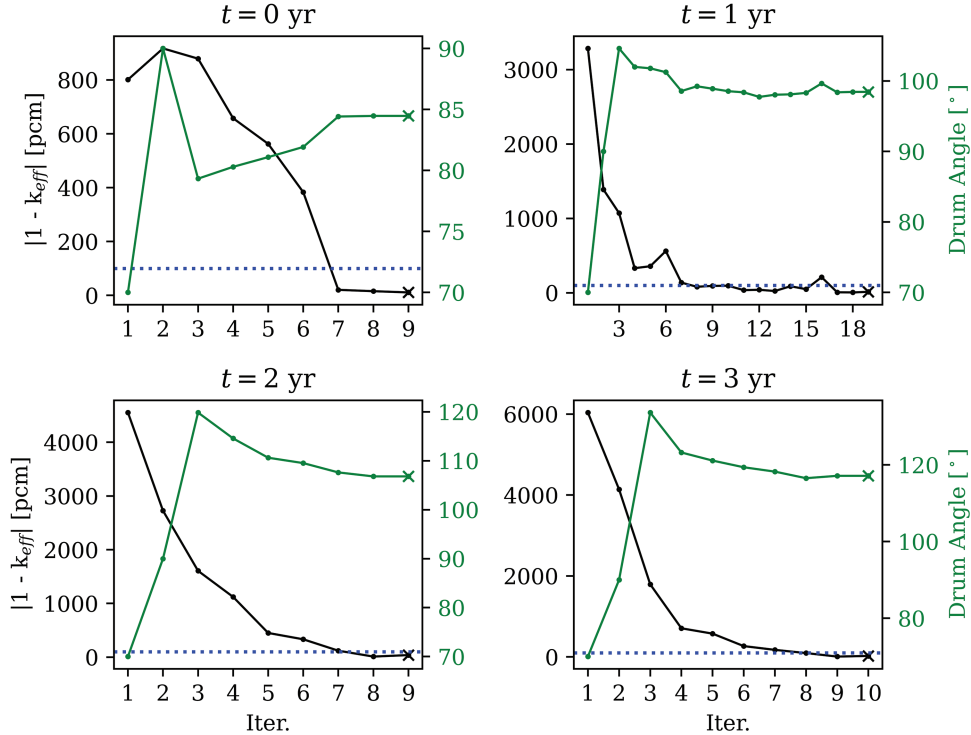


Fig. 10. Progression of critical control drum search with multiphysics coupling for reactor at different points in the core lifetime. The search termination criteria of 100 pcm in proximity to $k_{eff} = 1$ uncertainty are shown as blue dotted lines. The final iteration, indicated by “x” was executed without any update to the control drum position or Monte Carlo sampling parameters.

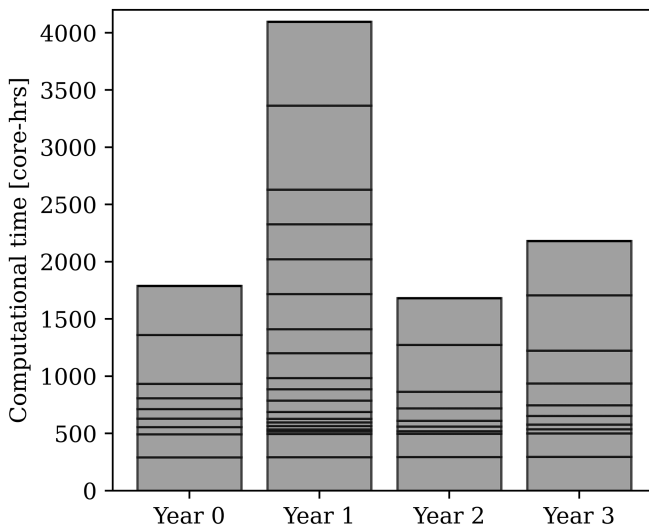


Fig. 11. Computational time dedicated to the transport solution step in the multiphysics coupling routine with critical control drum position search. Each bar represents the total time dedicated to a full coupling routine performed at a particular reactor time step. Divisions within each bar show how much time was dedicated to each iteration in the routine.

Additionally, subdivisions within each bar show how much computational time was dedicated to each step in the multiphysics simulation.

The two subdivisions at the bottom of each bar correspond to the first two iterations in each routine. These first two steps had user-provided Monte Carlo sampling parameters and control drum angles. Therefore, the computational time in these first two steps was the same across all search procedures. Then the GRsecant method selected the Monte Carlo sampling parameters and control drum angles for the remainder of the search until the last iteration. In the last iteration, the Monte Carlo sampling parameters were kept from the previous iteration. Therefore, the last two iterations within each of these four search routines had identical run times. Also note how, following the first two iterations, the GRsecant method ran faster calculations. As the search progressed and the core got closer to critical, the GRsecant method tended to run longer calculations until the target uncertainty in k_{eff} was achieved.

III.C. Fresh Core Characteristics

As conventional multiphysics simulation methodologies for microreactors may not model control drums in their critical position, Fig. 12 is provided to show a comparison between the core temperature distribution calculated with control drums fully withdrawn and one calculated with control drums in their critical position at BOL. Here, if

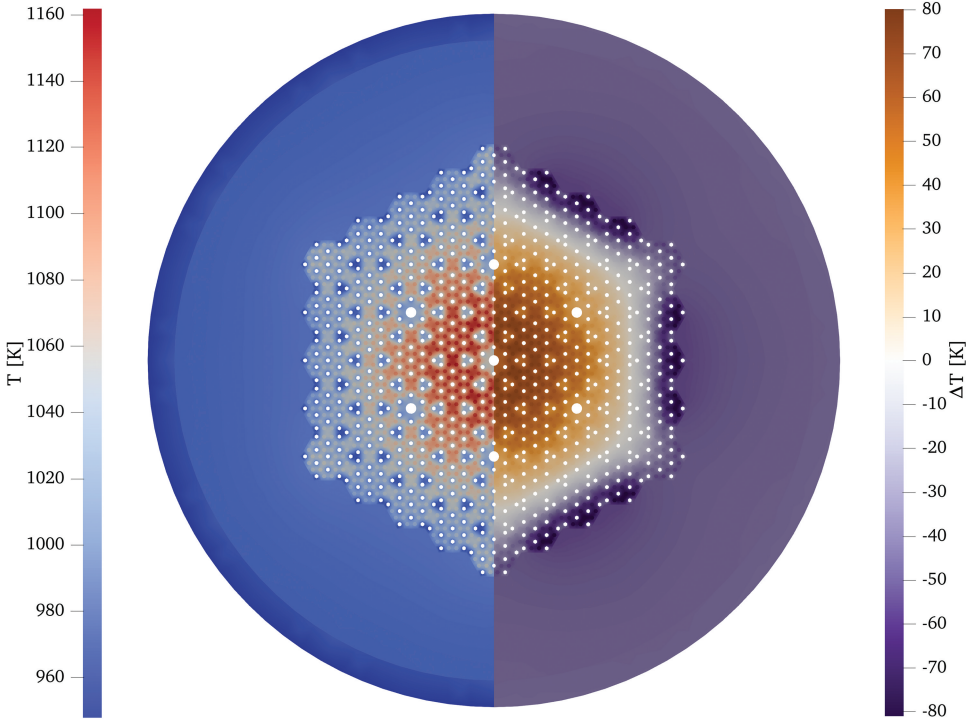


Fig. 12. (left) Core temperature distribution for core with drums in critical position and (right) difference between core temperature distributions with drums in critical position versus fully withdrawn, $\Delta T = T_{\text{critical}} - T_{\text{withdrawn}}$.

T_{critical} is used to represent the temperatures associated with the core when the control drums are in their critical position and $T_{\text{withdrawn}}$ for when the control drums are in their fully withdrawn positions, $\Delta T = T_{\text{critical}} - T_{\text{withdrawn}}$.

Qualitatively, the core temperature distribution with control drums in their critical positions closely resembles the core temperature distribution associated with the control drums fully inserted with the higher temperatures in the center of the core. Although this observation will likely become invalid for core temperature distributions later in the cycle, this leads to temperatures in the center of the core being underestimated compared to the model with control drums fully withdrawn. The high-temperature regions along the edge of the fueled region are also not present in the model with control drums in their critical position.

Table I provides a few design-relevant quantities associated with the EMD calculated with the multiphysics coupling routine with the control drums in their critical position, fully inserted, and fully withdrawn. As the critical drum position is nearly halfway between fully inserted and fully withdrawn, most calculated quantities associated with the critical drum position are between those calculated with the other two drum positions.

The one exception to this is the pin PF, which is the lowest for the case where the control drums are in their critical position. As previously seen in Fig. 7, this is

caused by a flatter pin power distribution that is not as center peaked as the distribution associated with the control drums fully inserted and not as peaked along the core periphery as the distribution associated with the control drums fully withdrawn. The pin power distribution calculated with control drums in their critical positions is shown in Fig. 13, where the radial distributions are certainly flatter than those shown in Fig. 7.

III.D. Method Application for Burnup Calculation

This final section provides results relevant to the burnup analysis of the EMD. So far, all results have focused on the methods discussed in Sec. II.D.1. For this section, the methods discussed in Sec. II.D.2 are employed to perform depletion calculations with approximately critical control drum positions. More specifically, the burnup calculations begin with fresh fuel by executing a multiphysics routine with critical control drum search. Then this control drum position and temperature distribution are set constant for a year-long depletion period, which was selected to balance computational cost and accuracy.

Using the terminology presented in Fig. 5, a standalone transport calculation was run halfway through the year-long depletion period to update the cellwise reaction rates without updating the control drum position or temperature

TABLE I
Comparison of Design Relevant Quantities Calculated with a Multiphysics Coupling Procedure for Three Control Drum Positions at BOL

	Drums Critical	Drums Inserted	Drums Withdrawn
Drum angle (deg)	84.5	0	180.
k_{eff}	1.00011	0.94357	1.09401
Pin PF	1.41	1.71	1.57
Pipe PF	1.37	1.61	1.18
Maximum fuel temperature (K)	1187	1263	1117
Maximum moderator temperature (K)	1175	1248	1101
Maximum vapor temperature (K) ^a	988	1024	959

^aMaximum vapor temperature refers to the maximum heat pipe vapor temperature in the core.

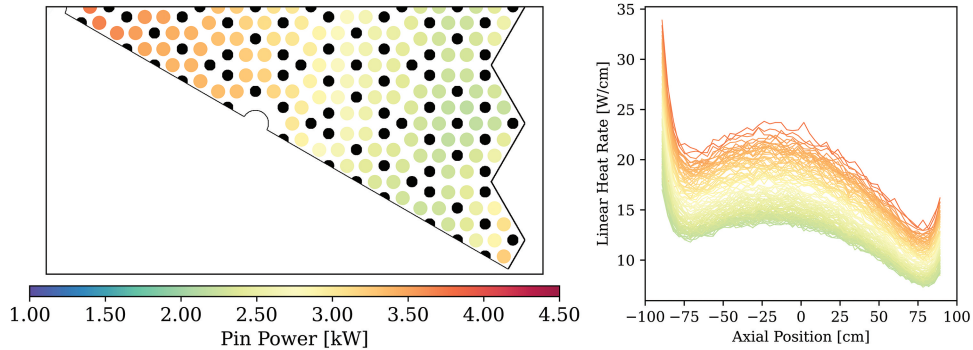


Fig. 13. Radial and axial power distributions calculated with the multiphysics coupling routine executed with critical drum position search. The limits on the pin power color bar are maintained from the limits used in Fig. 7.

distribution. The exception to this procedure occurred in the first step, where an additional burnup step was used to ensure equilibrium in the short-timescale isotopic behavior of the fuel. The resulting k_{eff} and control drum angle are shown in Fig. 14.

From the results shown in Fig. 14, the control drums began at 84.5 deg and were withdrawn over the cycle. Each point where a critical control drum search routine was performed, k_{eff} returned to a nearly critical value and proceeded to decrease over the course of the year. As the EMD contained no burnable poisons, the trend of the control drum angle and k_{eff} was relatively straightforward, but this would not be the case for all microreactor designs^[27] that may contain burnable poisons.

One additional piece of analysis that could be done with the results shown in Fig. 14 was to compare them to a depletion calculation that had a significantly lower computational cost and evaluate the impact on the estimated core lifetime. Namely, the multiphysics coupling routine could be executed on a core with fresh fuel and control drums fixed in their fully withdrawn position. Then, this same temperature distribution could be used

across the entirety of the core lifetime. In Fig. 15, the k_{eff} associated with this method is shown as “fresh T dist.” and compared with the results calculated with periodic critical control drum position searches. Additionally, following the 4 years of depletion shown in Fig. 14, the control drums were fully withdrawn and an additional year of depletion calculations were run.

Linear extrapolation on the last three data points were used to estimate the core lifetimes of each of these methods. From this, the core lifetime estimate resulting from the periodic critical position updates was 5.76 years, where the lifetime estimate resulting from the fixed control drum position was 5.83 years. This was only a difference of around 22 days. If core lifetime was the sole quantity of interest, this would be sufficient to avoid running periodic control drum position and temperature distribution update routines.

III.E. Core Burnup Behavior

In this section, more results on the behavior of the core during burnup are reported. These results are less

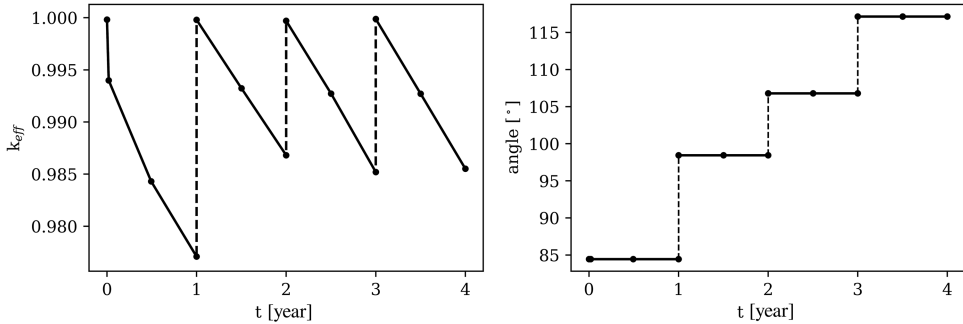


Fig. 14. Core k_{eff} and control drum position over a 4-year depletion calculation. Critical control drum position and core temperature distribution were updated every year. Points in line indicate times where the cellwise reaction rates were updated in the depletion routine.

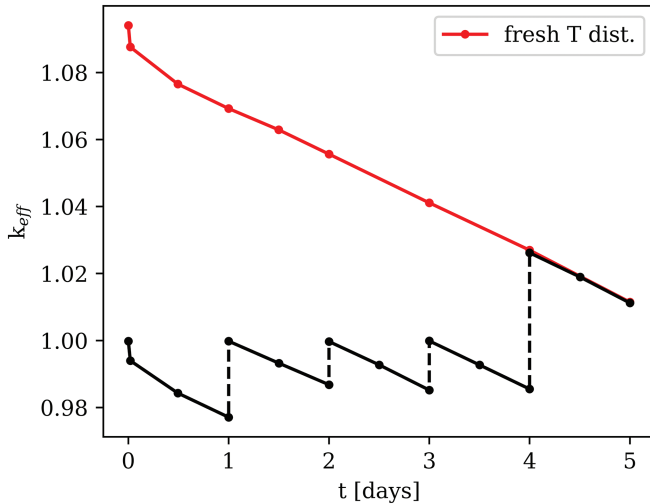


Fig. 15. Core k_{eff} associated with two methods for calculating the core lifetime. The results labeled as “fresh T dist.” were calculated with control drums fixed in the fully withdrawn position and the fresh fuel temperature distribution.

relevant to the performance of the coupling methodology and more relevant to the physical behavior of the reactor system. First, Fig. 16 shows both the end of life (EOL) temperature distribution of the core as well as a comparison to the core temperature distribution at BOL. In this figure, if T_{EOL} and T_{BOL} represent the core temperature distribution at EOL and BOL, respectively, then $\Delta T = T_{EOL} - T_{BOL}$. In this figure, the core temperature distribution at EOL tends to be flatter than at BOL. As this design has no burnable absorbers, the more rapid depletion of the high-power regions of the core will tend to flatten core temperature distributions.

This effect was additionally observed in Fig. 17, where the maximum core temperatures tend to decrease over the cycle. Also shown in this figure are the pin and pipe PFs. The pins on the periphery of the core tend to

increase in power because they benefit from three effects: (1) the removal of the control drum absorbing material, (2) proximity to the beryllium reflector, and (3) lower burnup due to control drum positions earlier in the cycle. This leads to the pin PF increasing as the cycle progresses and the control drums are removed. On the other hand, the pipe PF tends to consistently decrease because, as mentioned earlier, these pipes at the core edge are not surrounded by fuel pins.

IV. CONCLUSIONS

This work presented a multiphysics modeling methodology for heat pipe microreactors that includes a search for critical control drum position. The incorporation of this critical control drum position search procedure into the multiphysics coupling methodology permits the simultaneous convergence of the multiphysics solution and the critical control drum position. This novel aspect of the methodology enables performance of depletion calculations with critical control drum positions that account for multiphysics feedback.

Additionally, the stability of the multiphysics coupling procedure was discussed and analyzed in its application to the EMD microreactor. The main potential source of instability comes from the uncertainty in the calculated core k_{eff} values that arise from the Monte Carlo calculation method. These errors can cause erratic behavior in the selection of control drum positions during the critical position search. However, this instability was not observed to have a significant negative effect on the performance of the methodology. All multiphysics coupling routines that include a critical control drum search generally demonstrated monotonic convergence to steady-state operation with critical control drum positions. Even if this instability were severe,

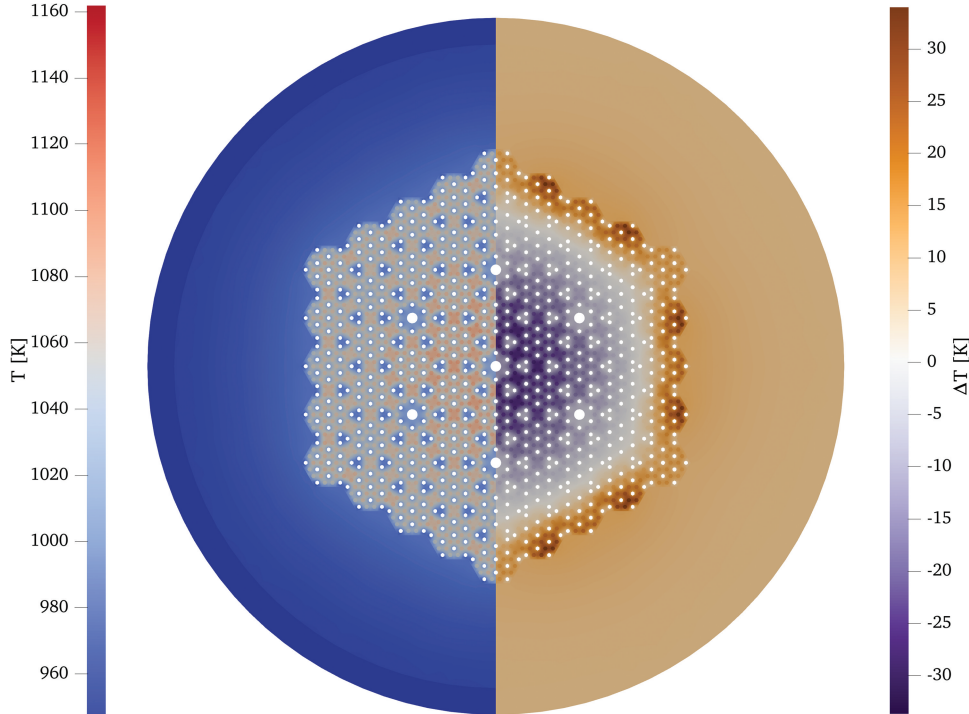


Fig. 16. (left) Core temperature distribution for core with drums in critical position at the end of cycle and (right) difference between the core temperature distributions with drums in critical position at BOL versus EOL, $\Delta T = T_{\text{EOL}} - T_{\text{BOL}}$.

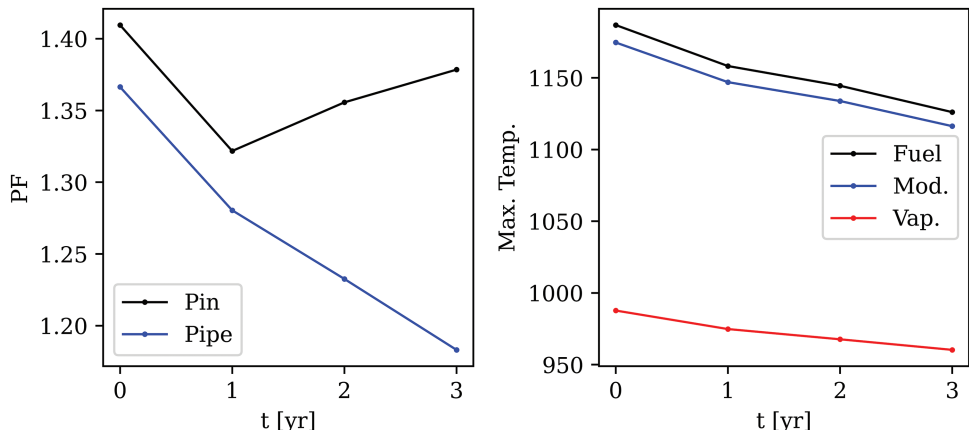


Fig. 17. Behavior of PFs and maximum core temperature distributions during core depletion. “Vap.” is used to refer to the heat pipe vapor core temperatures.

the bounded nature of the control drum position would prevent divergence.

Moving forward, significant differences in the pin power distribution were observed between the core with control drums fully inserted and fully withdrawn. At BOL, the pin power distribution with critical drum positions more resembled the center-peaking behavior of the core with control drums fully inserted than the edge-peaking behavior of the core with control drums fully withdrawn. Additionally, the total control drum worth

was compared between a calculation that included thermal feedback and one that did not, with only about a 1.5% difference observed between the two.

This multiphysics coupling procedure could be integrated into a burnup analysis by periodically updating the critical control drum positions and temperature distributions and updating the cellwise reaction rates. These periodic updates on the critical control drum positions and temperature distributions would require execution of the steady-state multiphysics coupling procedure.

The results from core depletion with critical drum positions were presented. Additionally, core lifetime estimates were compared between a calculation that periodically updated control drum positions and temperature distributions and one that only used the temperature distribution at BOL with control drums fully withdrawn. The difference between the lifetime estimates resulting from these two calculation methods was calculated to be small, around 1.5%.

The results and methodology demonstrated in this paper can aid heat pipe microreactor design efforts in the evaluation of the need for, and the impact of, multi-physics feedback in modeling calculations. The use of a Monte Carlo solution method for the neutron transport equation avoids the need for cross-section generation calculations. However, the steady-state reactor configurations calculated from this methodology can certainly be used for the generation of cross sections required by other simulation tools, such as DireWolf.

Disclosure Statement

No potential competing interest was reported by the authors.

Funding

This material is based on work supported under a U.S. Department of Energy, Office of Nuclear Energy, Integrated University Program Graduate Fellowship. This research made use of the Idaho National Laboratory computing resources, which are supported by the Office of Nuclear Energy of the U.S. Department of Energy and the Nuclear Science User Facilities under contract no. DE-AC07-05ID14517.

Credit Statement

Dean Price: Conceptualization, methodology, software, investigation, writing—original draft, and visualization. Nathan Roskoff: Conceptualization, resources, writing—review and editing, and supervision. Majdi Radaideh: Conceptualization, writing—review and editing, and supervision. Brendan Kochunas: Conceptualization, writing—review and editing, supervision, and funding acquisition.

Acronyms

BOL = beginning of life

EMD = eVinci motivated design

EOL = end of life

LWR = light water reactor

MOOSE = Multiphysics Object Oriented Simulation Environment

PF = peaking factor

SIMPLE = semi-implicit method for pressure-linked equations

TRISO = tri-structural isotropic

ORCID

Dean Price  <http://orcid.org/0000-0003-0999-0111>
Majdi I. Radaideh  <http://orcid.org/0000-0002-2743-0567>

Brendan Kochunas  <http://orcid.org/0000-0001-7109-9368>

References

1. G. BLACK et al., “Prospects for Nuclear Microreactors: A Review of the Technology, Economics, and Regulatory Considerations,” *Nucl. Technol.*, **209**, S1 (2022); <https://doi.org/10.1080/00295450.2022.2118626>.
2. D. GASTON et al., “Parallel Multi-Physics Algorithms and Software for Computational Nuclear Engineering,” *Journal of Physics: Conference Series*, **180**, 012012, IOP Publishing (2009).
3. C. J. PERMANN et al., “MOOSE: Enabling Massively Parallel Multiphysics Simulation,” *SoftwareX*, **11**, 100430 (2020); <https://doi.org/10.1016/j.softx.2020.100430>.
4. C. MATTHEWS et al., “Coupled Multiphysics Simulations of Heat Pipe Microreactors Using DireWolf,” *Nucl. Technol.*, **207**, 7, 1142 (2021); <https://doi.org/10.1080/00295450.2021.1906474>.
5. Y. WANG et al., “Rattlesnake: A MOOSE-Based Multiphysics Multischeme Radiation Transport Application,” *Nucl. Technol.*, **207**, 7, 1047 (2021); <https://doi.org/10.1080/00295450.2020.1843348>.
6. F. KONG et al., “A Highly Parallel Multilevel Newton-Krylov-Schwarz Method with Subspace-Based Coarsening and Partition-Based Balancing for the Multigroup Neutron Transport Equation on Three-Dimensional Unstructured Meshes,” *SIAM J. Sci. Comput.*, **42**, 5, C193 (2020); <https://doi.org/10.1137/19M1249060>.
7. Z. M. PRINCE and J. C. RAGUSA, “Multiphysics Reactor-Core Simulations Using the Improved Quasi-Static Method,” *Ann. Nucl. Energy*, **125**, 186 (2019); <https://doi.org/10.1016/j.anucene.2018.10.056>.
8. J. LEPPÄNEN et al., “The Serpent Monte Carlo Code: Status, Development and Applications in 2013,” *Ann. Nucl. Energy*, **82**, 142 (2015); <https://doi.org/10.1016/j.anucene.2014.08.024>.

9. R. A. BERRY et al., “Sockeye Heat Pipe Code Theory Development: Based on the 7-Equation, Two-Phase Flow Model of RELAP-7,” Technical Report, Idaho National Laboratory (2019).
10. C. MUELLER and P. TSVETKOV, “A Review of Heat-Pipe Modeling and Simulation Approaches in Nuclear Systems Design and Analysis,” *Ann. Nucl. Energy*, **160**, 108393 (2021); <https://doi.org/10.1016/j.anucene.2021.108393>.
11. R. L. WILLIAMSON et al., “Multidimensional Multiphysics Simulation of Nuclear Fuel Behavior,” *J. Nucl. Mater.*, **423**, 1–3, 149 (2012); <https://doi.org/10.1016/j.jnucmat.2012.01.012>.
12. A. FALLGREN, D. RAO, and H. TRELLUE, “Heatpipe Reactor Design for Special Purpose Applications,” Los Alamos National Laboratory (2018).
13. N. ROSKOFF et al., “Madeleine Charlot, Modeling and Analysis of a Micro-Reactor Using the DireWolf Code Suite,” Technical Report, Idaho National Laboratory (2022).
14. N. ROSKOFF, V. KUCUKBOYACI, and A. LEVINSKY, “Transient Analysis of a Micro-Reactor Using the DireWolf Code Suite,” *Proc. int. Conf. on Physics of Reactors (PHYSOR 2022)* (2022).
15. B. KOCHUNAS et al., “VERA Core Simulator Methodology for Pressurized Water Reactor Cycle Depletion,” *Nucl. Sci. Eng.*, **185**, 1, 217 (2017); <https://doi.org/10.13182/NSE16-39>.
16. B. COLLINS et al., “Stability and Accuracy of 3D Neutron Transport Simulations Using the 2D/1D Method in MPACT,” *J. Comput. Phys.*, **326**, 612 (2016); <https://doi.org/10.1016/j.jcp.2016.08.022>.
17. Y. S. JUNG et al., “Practical Numerical Reactor Employing Direct Whole Core Neutron Transport and Subchannel Thermal/Hydraulic Solvers,” *Ann. Nucl. Energy*, **62**, 357 (2013); <https://doi.org/10.1016/j.anucene.2013.06.031>.
18. C. CASTAGNA et al., “A Serpent/Open-FOAM Coupling for 3D Burnup Analysis,” *Eur. Phys. J. Plus*, **135**, 5, 433 (2020).
19. D. KOTLYAR and E. SHWAGERAUS, “Monitoring and Preventing Numerical Oscillations in 3D Simulations with Coupled Monte Carlo Codes,” *Ann. Nucl. Energy*, **71**, 198 (2014); <https://doi.org/10.1016/j.anucene.2014.04.002>.
20. D. F. GILL, D. P. GRIESHEIMER, and D. L. AUMILLER, “Numerical Methods in Coupled Monte Carlo and Thermal-Hydraulic Calculations,” *Nucl. Sci. Eng.*, **185**, 1, 194 (2017); <https://doi.org/10.13182/NSE16-3>.
21. J. DUFEK and J. E. HOOGENBOOM, “Numerical Stability of Existing Monte Carlo Burnup Codes in Cycle Calculations of Critical Reactors,” *Nucl. Sci. Eng.*, **162**, 3, 307 (2009); <https://doi.org/10.13182/NSE08-69TN>.
22. J. IM et al., “Multiphysics Analysis System for Heat Pipe Cooled Micro Reactors Employing PRAGMA-OpenFOAM-ANLHTP,” *Nucl. Sci. Eng.*, **197**, 8, 1743 (2023); <https://doi.org/10.1080/00295639.2022.2143209>.
23. V. K. MEHTA et al., “Capturing Multiphysics Effects in Hydride Moderated Microreactors Using MARM,” *Ann. Nucl. Energy*, **172**, 109067 (2022); <https://doi.org/10.1016/j.anucene.2022.109067>.
24. T. LI et al., “Multi-Physics Coupled Simulation on Steady-State and Transients of Heat Pipe Cooled Reactor System,” *Ann. Nucl. Energy*, **187**, 109774 (2023); <https://doi.org/10.1016/j.anucene.2023.109774>.
25. A. NOVAK et al., “Multiphysics Coupling of OpenMC CAD-Based Transport to MOOSE Using Cardinal and Aurora,” *Proc. M&C* (2023).
26. M. E. ABBASSI, D. LAHAYE, and K. VUIK, “Modelling Turbulent Combustion Coupled with Conjugate Heat Transfer in OpenFOAM,” *Proc. Numerical Mathematics and Advanced Applications ENUMATH 2019: European Conference*, p. 1137, Egmond aan Zee, The Netherlands, September 30–October 4, 2019, Springer (2020).
27. D. PRICE and N. ROSKOFF, “Method for Control Drum Position Critical Search with Monte Carlo Codes,” *Prog. Nucl. Energy*, **162**, 104731 (2023); <https://doi.org/10.1016/j.pnucene.2023.104731>.
28. Y. ARAFAT and J. van WYK, “eVinci Micro Reactor,” *Nucl. Plant J.*, **37**, 34 (2019).
29. D. PRICE et al., “Thermal Modeling of an eVinci™-Like Heat Pipe Microreactor Using OpenFOAM,” *Nucl. Eng. Des.*, **415**, 112709 (2023); <https://doi.org/10.1016/j.nucengdes.2023.112709>.
30. A. M. COX et al., “Monte Carlo Methods for the Neutron Transport Equation,” *SIAM/ASA J. Uncertainty Quantif.*, **10**, 2, 775 (2022); <https://doi.org/10.1137/21M1390578>.
31. S. S. CHIRAYATH, C. R. SCHAFER, and G. R. LONG, “A New Methodology to Estimate Stochastic Uncertainty of MCNP-Predicted Isotope Concentrations in Nuclear Fuel Burnup Simulations,” *Ann. Nucl. Energy*, **151**, 107911 (2021); <https://doi.org/10.1016/j.anucene.2020.107911>.
32. N. GARCIA-HERRANZ et al., “Propagation of Statistical and Nuclear Data Uncertainties in Monte Carlo Burn-Up Calculations,” *Ann. Nucl. Energy*, **35**, 4, 714 (2008); <https://doi.org/10.1016/j.anucene.2007.07.022>.
33. T. TAKEDA, N. HIROKAWA, and T. NODA, “Estimation of Error Propagation in Monte-Carlo Burnup Calculations,” *J. Nucl. Sci. Technol.*, **36**, 9, 738 (1999); <https://doi.org/10.1080/18811248.1999.9726262>.
34. M. TOHJOH et al., “Effect of Error Propagation of Nuclide Number Densities on Monte Carlo Burn-Up Calculations,” *Ann. Nucl. Energy*, **33**, 17–18, 1424 (2006); <https://doi.org/10.1016/j.anucene.2006.09.010>.
35. E. DUMONTEIL and C. DIOP, “Biases and Statistical Errors in Monte Carlo Burnup Calculations: An Unbiased

- Stochastic Scheme to Solve Boltzmann/Bateman Coupled Equations,” *Nucl. Sci. Eng.*, **167**, 2, 165 (2011); <https://doi.org/10.13182/NSE09-100>.
36. M. B. CHADWICK et al., “ENDF/B-VII. 1 Nuclear Data for Science and Technology: Cross Sections, Covariances, Fission Product Yields and Decay Data,” *Nucl. Data Sheets*, **112**, 12, 2887 (2011); <https://doi.org/10.1016/j.nds.2011.11.002>.
37. S. V. PATANKAR, *Numerical Heat Transfer and Fluid Flow*, CRC Press (2018).
38. C. GEUZAIN and J.-F. REMACLE, “Gmsh: A 3-D Finite Element Mesh Generator with Built-In Pre-and Post-Processing Facilities,” *Int. J. Numer. Methods Eng.*, **79**, 11, 1309 (2009); <https://doi.org/10.1002/nme.2579>.
39. J. H. LIENHARD, *A Heat Transfer Textbook*, Phlogiston (2005).
40. C. WANG et al., “Performance Analysis of Heat Pipe Radiator Unit for Space Nuclear Power Reactor,” *Ann. Nucl. Energy*, **103**, 74 (2017); <https://doi.org/10.1016/j.anucene.2017.01.015>.